Pergamon

SCIENCE DIRECT®

Bioorganic & Medicinal Chemistry 11 (2003) 3359–3366

BIOORGANIC & MEDICINAL CHEMISTRY

Comparison between Gd-DTPA and Several Bisamide Derivatives as Potential MRI Contrast Agents

Jianghua Feng,[a] Guoying Sun,[a] Fengkui Pei[a,*] and Maili Liu[b]

[a]*Changchun Institute of Applied Chemistry, Chinese Academy of Sciences, Changchun, 130022, PR China*
[b]*Laboratory of Magnetic Resonance and Atomic and Molecular Physics, Wuhan Institute of Physics and Mathematics, Chinese Academy of Sciences, Wuhan, 430071, PR China*

Received 6 December 2002; revised 10 January 2003; accepted 14 January 2003

Abstract—Four neutral gadolinium complexes of diethylenetriaminepentaacetic acid (DTPA)-bisamide derivatives have been synthesized and characterized. Their potential application as tissue-specific and low-osmolarity MRI contrast agents has been evaluated by in vitro and in vivo experiments. Their measured relaxivities in D_2O, bovine serum albumin and human serum transferrin solutions showed favorable relaxation ability. In vivo studies have proven that Gd(DTPA–BDMA), Gd(DTPA–BIN), and Gd(cyclic-DTPA–1,2-pn) could be promising liver-specific MRI contrast agents and Gd(DTPA–BDMA), and Gd(cyclic-DTPA–1,2-pn) have favorable renal excretion capability. Among them, Gd(cyclic-DTPA–1,2-pn) is a more powerful hepatic contrast agent and Gd(DTPA–BIN) provides the stable imaging contrast for several hours. They also show a lower toxicity.

Introduction

It is well known that magnetic resonance imaging (MRI) is a non-invasive and efficient imaging technique. Prior to MRI diagnosis, certain agents, so-called contrast agents (CAs), might be administrated in ca. 35% examinations to further enhance the imaging contrasts between normal and abnormal tissues, or to reveal the pathological conditions, such as tumors and tissue damage.[1] Current CAs in clinical use are essentially gadolinium complexes, such as gadopentetate dimeglumine, gadoteridol, gadodiamide, and gadoterate meglumine.[2,3] They enhance various portions of the MR image by changing, usually increasing, the relaxation rate of bulk water protons in close vicinity of the agent, thus allowing the region of interest to be much more conspicuous than the surrounding tissue.[1,4] Continuing interest in the developing of efficient, low-toxic, and target-specific contrast agents for in vivo image enhancement has led to the preparation and study of a wide range of complexes in last two decades.[5–16] Among them, Gd-DTPA (gadolinium-diethylenetriaminepentaacetic acid) and its derivatives have been successfully used in clinical MRI due to their thermodynamic stabilities, kinetic inertnesses, high relaxivities and potential target specificities after certain modification.[4,17–23] However, most of gadolinium complexes are charged salts under physiological conditions, therefore, the required counterions increase the osmolality of the solution. Minimum osmolality is predicted for a neutral complex because it exists as a single particle in aqueous solution.[24–27] Here reported are the syntheses, animal test on toxicity and MRI imaging evaluations of four neutral Gd-DTPA bis(amide) derivatives (structures shown in Fig. 7): Gd(DTPA–BDMA) (gadolinium-[(2-{carboxymethyl-[2-(carboxymethyl-dimethylcarbamoyl-methyl-amino)-ethyl]-amino}-ethyl)-dimethylcarbamoyl-methyl-amino]-acetic acid), Gd(DTPA–BDEA) (gadolinium-[(2-{carboxymethyl-[2-(carboxymethyl-diethylcarbamoylmethyl-amino)-ethyl]-amino}-ethyl)-diethylcarbamoylmethyl-amino]-acetic acid), Gd(DTPA–BIN) (gadolinium-((2-{carboxymethyl-[2-(carboxymethyl-{2-oxo-2-[*N*′-(pyridine-4-carbonyl)-hydrazino]-ethyl}-amino)-ethyl]-amino}-ethyl)-{2-oxo-2-[*N*′-(pyridine-4-carbonyl)-hydrazino]-ethyl}-amino)-acetic acid), and Gd(cyclic-DTPA–1,2-pn) (gadolinium-(10,13-bis-carboxymethyl-6-methyl-3,8-dioxo-1,4,7,10,13pentaaza- cyclopentadec-1-yl)-acetic acid).

Results

For paramagnetic aqueous solution, the solvent longitudinal relaxation rate, $1/T_{1obsd}$, is linearly dependent

*Corresponding author. Tel.: +86-431-526-2219; fax: +86-431-568-5653; e-mail: peifk@ciac.jl.cn

0968-0896/03/$ - see front matter © 2003 Elsevier Science Ltd. All rights reserved.
doi:10.1016/S0968-0896(03)00263-3

Table 1. The T_1-relaxivities and LD_{50} of Gd-DTPA and its four bisamide derivatives

Gadolinium complexes	The T_1-relaxivities R_1 ($mM^{-1}\cdot s^{-1}$)			LD_{50} (mmol/kg)
	in D_2O	in 0.725 mmol·L^{-1} BSA	in 35 μmol·L^{-1} hTF	
GdDTPA	5.25	~5.40[a]	—	6~10
Gd(DTPA–BDMA)	4.01	4.34	4.82	—
Gd(DTPA–BDEA)	4.97	4.96	3.60	3.2
Gd(DTPA–BIN)	3.28	~3.33[a]	~3.38[a]	2.9
Gd(cyclic-DTPA–1,2-pn)	7.11	8.31	10.20	2.0

[a]The relaxivity obtained from the linear regression according to eq 1 described in the text.

on the concentration of the paramagnetic species ([CA]) as described in eq 1:

$$\frac{1}{T_{1obsd}} = r_1 \times [CA] + \frac{1}{T_{1dia}} \quad (1)$$

where $1/T_{1obsd}$ and $1/T_{1dia}$ are the measured solvent relaxation rate in the presence and absence of the paramagnetic species, respectively, and r_1 is the relaxivity in units of $mM^{-1}\cdot s^{-1}$, which reflects the relaxation enhancement ability of a paramagnetic compound.

The T_1-relaxivities of the four Gd-DTPA bisamide derivatives in D_2O, 0.725 mmol·L^{-1} BSA, and 35 μmol·L^{-1} hTF solutions were listed in Table 1. T_1-relaxivities of Gd(DTPA–BDMA), Gd(DTPA–BDEA), and Gd(DTPA–BIN) are similar to that of Gd(DTPA), while T_1-relaxivity of Gd(cyclic-DTPA–1,2-pn) is higher than that of Gd(DTPA), which may be due to the rigidity of its cyclic structure. Significant increases in relaxivity for Gd(DTPA–BDMA) and Gd(cyclic-DTPA–1,2-pn) in the presence of BSA and hTF were observed. However, the solvent longitudinal relaxation rates of Gd(DTPA–BIN) against concentration in both BSA and hTF solution can not be properly fitted by using a linear equation. Instead, they can be excellently fitted by using a second order polynomial equation with a correlation coefficient greater than 0.998, which is similar to GdDTPA in the presence of human serum albumin (HSA) and BSA.[28,29]

An intravenous LD_{50} of about 3.2, 2.9, and 2.0 mmol/kg body wt corresponding to Gd(DTPA–BDEA), Gd(DTPA–BIN), and Gd(cyclic-DTPA–1,2-pn) was estimated, respectively (Table 1). Death occurred within the first 12 h after injection, and no long-term toxicity and effects were seen for the survivors during the 14-day observation time.

Gd(DTPA–BDMA), Gd(DTPA–BDEA), Gd(DTPA–BIN), and Gd(cyclic-DTPA–1,2-pn) have been evaluated as magnetic resonance imaging contrast agents in SD rat liver and kidney. As shown in Figures 1–4, signal

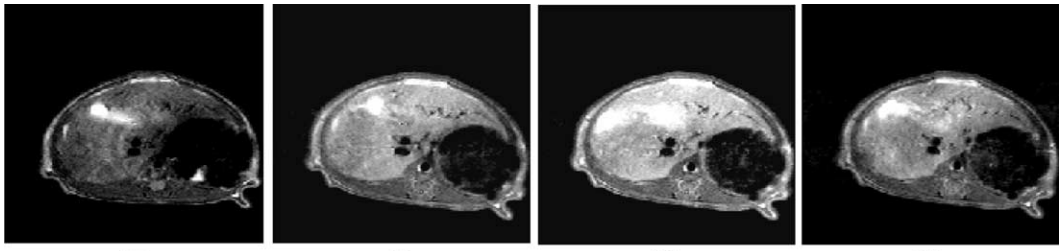

Figure 1. MR images of a transverse section of a Sprague–Dawley rat liver (the portions of left and top right in every image) using Gd(cyclic-DTPA–1,2-pn) as the contrast enhancement agent. Sections (1)–(4) are shown as follows: (1) control, prior to injection; (2) post-injection, 10 min; (3) post-injection, 35 min; (4) post-injection, 75 min.

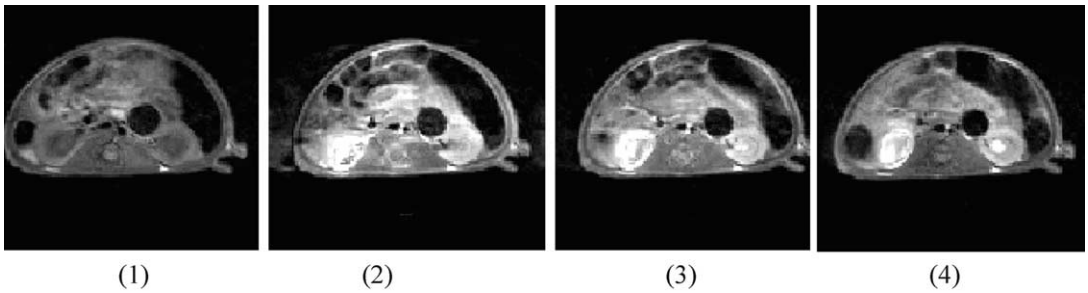

Figure 2. MR images of a transverse section of a Sprague–Dawley rat kidney (the two elliptic portions of the bottom left (right kidney) and the bottom right (left right) in every image) using Gd(DTPA–BDMA) as the contrast enhancement agent. Sections (1)–(4) are shown as follows: (1) control, prior to injection; (2) post-injection, 15 min; (3) post-injection, 30 min; (4) post-injection, 65 min.

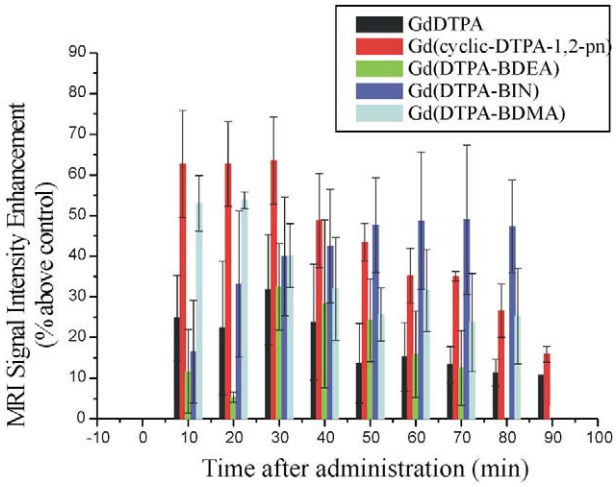

Figure 3. Time dependence of the contrast agents induced hepatic intensity enhancement obtained from the T_1-weighted images.

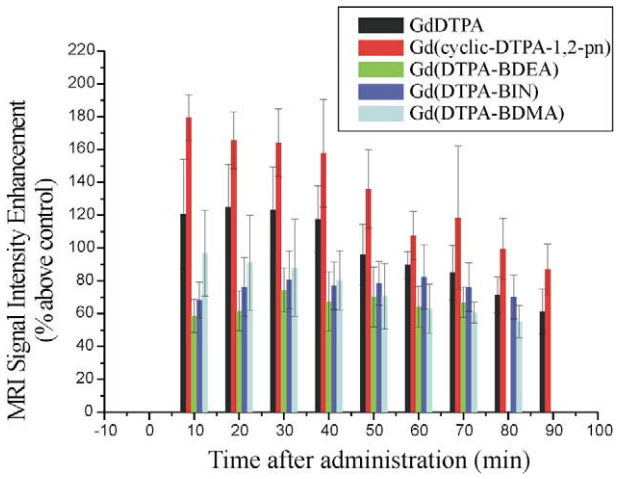

Figure 4. Time dependence of the contrast agents induced renal intensity enhancement obtained from the T_1-weighted images.

enhancement in the T_1-weighted image was obtained at abdomen after iv administration of contrast agents with the doses of 0.185±0.005, 0.193±0.006, 0.197±0.006, 0.197±0.016, and 0.175±0.015 mmol Gd/kg for Gd(DTPA), Gd(DTPA–BDMA), Gd(DTPA–BDEA), Gd(DTPA–BIN), and Gd(cyclic-DTPA–1,2-pn), respectively, which were around 2-fold of typical clinical dose (0.1 mmol Gd/kg).

The signal intensity of the rat liver parenchyma and kidney increased shortly after injection of Gd(cyclic-DTPA–1,2-pn). Fig. 1 showed the T_1-weighted image of the rat liver for precontrast and after application of Gd(cyclic-DTPA–1,2-pn). The maximum enhancement for liver was found in 5–40 min after injection (Fig. 3). The experimental dose of Gd(cyclic-DTPA–1,2-pn) induced 65.0±12.3% enhancement in signal intensity of the liver, and 168±20.5% enhancement for the kidney (Fig. 4). The signal intensity of the rat liver parenchyma increased slowly following administration of Gd(DTPA–BIN) and persisted stronger enhancement throughout the imaging period (Fig. 3). Gd(DTPA–BIN) induced 48.2±14.9% enhancement in signal intensity of the liver in 30–60 min after injection.

Both liver and kidney demonstrated early enhancement after iv injection of Gd(DTPA–BDMA) (Figs 2–4). The maximum percentage enhancement in liver (57.0±4.8%) appeared within 5–20 min, and decreased slowly thereafter. A mean percentage enhancement for kidney of close to 80% was reached within the first 30 min, and the enhancement persisted throughout the imaging period. As for Gd(DTPA–BDEA), the enhancement patterns of liver were very similar to Gd(DTPA): the maximum enhancements of 27.4±17.4% were found in 30∼40 min after injection and the enhancement decreased rapidly thereafter (Fig. 3). Compared with a mean percentage enhancement of 121±24.8% for Gd–DTPA for the kidney, the enhancement is weak with that of 70.3±16.6% for Gd(DTPA–BDEA) (Fig. 4).

There is a large variation of percentage enhancement values in liver and kidney between the rats as indicated by the large standard deviations (Figs 3 and 4), but the enhancement patterns were essentially the same in the different rats after injection of the same agent.

Discussion

Serum albumin is the richest protein of human blood plasma, and human serum transferrin (hTF) is the most important binding protein with lanthanide complex.[30] They would play a crucial role on the uptake, transportation, biodistribution and excretion of contrast agent in human body.[28] Significant enhancements of solvent proton relaxation rates were found for the Gd(DTPA–BDMA) and Gd(cyclic-DTPA–1,2-pn) in BSA and hTF solution, indicating the formation of paramagnetic macromolecular adducts.[9,31] It is very likely that Gd(DTPA–BDMA) and Gd(cyclic-DTPA–1,2-pn) formed a paramagnetic macromolecular adduct in the forms of [Gd-DTPA–bis(amide) derivatives]·BSA and [Gd-DTPA–bis(amide) derivatives]·hTF. While Gd(DTPA–BIN) integrates noncovalently with BSA and hTF in the forms of [Gd(DTPA–BIN)]·BSA, $[Gd(DTPA–BIN)]_2$·BSA and [Gd(DTPA–BIN)]·hTF, $[Gd(DTPA–BIN)]_2$·hTF. From the experimental data, we deduced that protein binding ratio of Gd(DTPA–BDMA) was 5.5% for BSA and 11.2% for hTF by using of the method in ref 28, and 13.5 and 29.0% for Gd(cyclic-DTPA–1,2-pn), respectively. While at most 1.08 and 0.24% of Gd(DTPA–BIN) exist as [Gd(DTPA–BIN)]·BSA and $[Gd(DTPA–BIN)]_2$·BSA, and 2.03 and 6.34% exist as [Gd(DTPA–BIN)]·hTF and $[Gd(DTPA–BIN)]_2$·hTF. An evident enhancement in the liver after injection of Gd(DTPA–BDMA), Gd(DTPA–BIN), and Gd(cyclic-DTPA–1,2-pn) is probably related to the protein binding with serum albumin and serum transferrin and thus, leading to effective transport by the blood to the liver. The data of relaxivities and the results of the in vivo MRI studies seem to indicate that

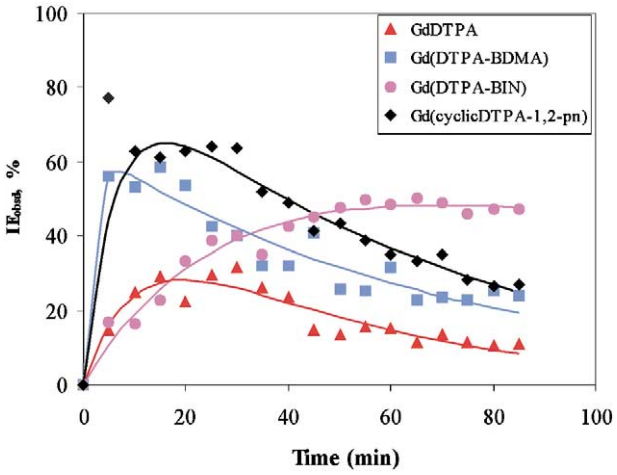

Figure 5. Time dependence of the contrast agents induced hepatic intensity enhancement obtained from the T_1-weighted images. The curves are the best fitted according to eq 3 described in the text.

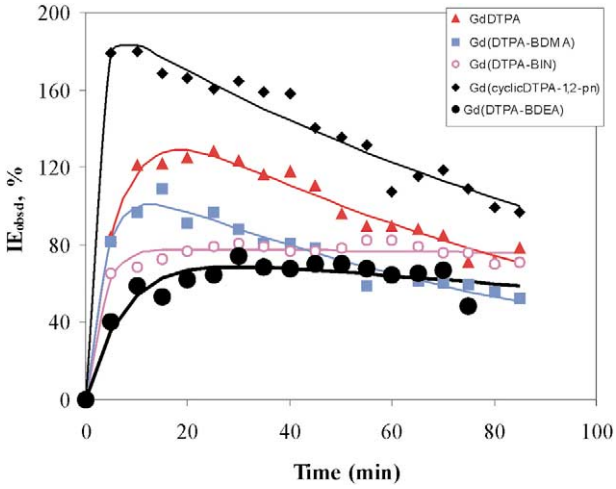

Figure 6. Time dependence of the contrast agents induced renal intensity enhancement obtained from the T_1-weighted images. The curves are the best fitted according to eq 3 described in the text.

hTF makes larger contribution than serum albumin in transporting the compounds in the body.

In contrast to the rapid metabolized rate of GdDTPA, for the animal group receiving Gd(DTPA–BDMA), Gd(DTPA–BIN), and Gd(cyclic-DTPA–1,2-pn) the peak enhancement in liver kept for a longer time.

Certainly, the uptake and excretion of contrast agents are very complex processes. However in our opinion, the signal intensity changes ultimately due to distribution (uptake) and elimination (excretion) of the contrast agents, whichever species they are in. To understand the properties of the complexes better, we assume that the uptake and the excretion of these agents follow a simplified model shown as eq 4 (see Experimental). Data shown in Figure 3 can be well fitted to the model except for Gd(DTPA–BDEA). For Gd(DTPA–BDEA), the mean IE_{obsd}'s at 10-25 min are abnormally low. Shown in Figure 5 are the fitting curves of other four Gd^{3+} complexes and listed in Table 2 are the corresponding parameters. The fact that IE_{max} of Gd(cyclic-DTPA–1,2-pn) is much larger than those of others indicates that this complex is more powerful hepatic contrast agents at its peak duration time (10–30 min). The parameters in Table 2 show that the hepatic uptake rates decrease in order of: Gd(DTPA–BDMA) ($t_{1/2,uptake}$ = 1.8 min) < Gd(cyclic-DTPA–1,2-pn) (6.2 min) < GdDTPA (10.3 min) ≪ Gd(DTPA–BIN) (27.4 min), and the hepatic excretion rates follow a slightly different order of: GdDTPA ($t_{1/2,\ excretion}$ = 44.5 min) < Gd(cyclic-DTPA–1,2-pn) (65.2 min) ≈ Gd(DTPA–BDMA) (70.4 min) ≪ Gd(DTPA–BIN) (263.3 min). Among them, Gd(DTPA–BIN) is the most particular one, which shows extremely slow hepatic excretion. This property may make it be a good selection as a hepatic contrast agent to provide stable imaging contrast for several hours! It provides a big advantage in comparison with the efficient time of contrast agents currently in clinical use, usually less than 1 h. Favorable enhancement in liver after injection probably supports that Gd(DTPA–BDMA), Gd(DTPA–BIN), and Gd(cyclic-DTPA–1,2-pn) were excreted, at least in part, through the hepatocytes into the bile and feces.

Besides the liver, kidney was significantly enhanced, indicating that the four GdDTPA bisamide derivatives were also being removed from the blood and eliminated through the kidney. Data shown in Figure 4 can be well fitted to the same model as liver as well. Shown in Figure 6 are the fitting curves of Gd^{3+} complexes and listed in Table 3 are the corresponding parameters. The parameters in Table 3 show that the renal uptake rates decrease in order of: Gd(cyclic-DTPA–1,2-pn) ($t_{1/2,\ uptake}$ = 1.9 min) < Gd(DTPA–BIN) (3.2 min) < Gd(DTPA–BDMA) (3.8 min) < GdDTPA (6.2 min)

Table 2. The half lifetimes of hepatic uptake and excretion of GdDTPA and bis(amide) derivatives

Gd^{3+} complexes	IE_{max}[a]	$t_{1/2}$, uptake[b] min	$t_{1/2}$, excretion min	AF[c]
GdDTPA	57.3	10.3	44.5	0.15
Gd(DTPA–BDMA)	64.3	1.8	70.4	0.12
Gd(DTPA–BIN)	70.0	27.4	263.3	0.06
Gd(cyclic-DTPA–1,2-pn)	92.0	6.2	65.2	0.06

[a] IE_{max} is the maximum value available of intensity enhancement for liver after administration of contrast agent.
[b] The uptake and excretion time was calculated by using Solver of the option of Excel 2002 (Microsoft Corp.) according to non-linear programming.
[c] AF represents the agreement factor between the experimental and calculated hepatic excretion curve showed in Figure 6, which is defined as follows: $AF = \sqrt{\frac{\sum (IE_{exp} - IE_{cal})^2}{\sum IE_{exp}^2}}$ where IE_{exp} and IE_{cal} are the experimental and calculated intensity enhancements, respectively.

Table 3. The half lifetimes of renal uptake and excretion of GdDTPA and bis(amide) derivatives

Gd^{3+} complexes	IE_{max}[a]	$t_{1/2}$, uptake[b] min	$t_{1/2}$, excretion min	AF[c]
GdDTPA	165.7	6.2	99.8	0.04
Gd(DTPA–BDMA)	119.2	3.8	98.9	0.05
Gd(DTPA–BDEA)	77.91	7.8	305.2	0.08
Gd(DTPA–BIN)	78.6	3.2	2265.4	0.05
Gd(cyclic-DTPA–1,2-pn)	199.7	1.9	123.3	0.05

[a]IE_{max} is the maximum value available of intensity enhancement for kidney after administration of contrast agent.
[b]The uptake and excretion time was calculated by using Solver of the option of Excel 2002 (Microsoft Corp.) according to non-linear programming.
[c]AF represents the agreement factor between the experimental and calculated renal excretion curve, which is defined as follows:
$AF = \sqrt{\frac{\sum (IE_{exp} - IE_{cal})^2}{\sum IE_{exp}^2}}$ where IE_{exp} and IE_{cal} are the experimental and calculated intensity enhancements, respectively.

< Gd(DTPA–BDEA) (7.8 min), and the renal excretion rates follow a different order of: Gd(DTPA–BDMA) ($t_{1/2,excretion}$ = 98.9 min)≈GdDTPA (99.8 min) < Gd(cyclic-DTPA–1,2-pn) (123.3 min) < Gd(DTPA–BDEA) (305.2 min)≪Gd(DTPA–BIN) (2265.4 min). IE_{max} of Gd(cyclic-DTPA–1,2-pn) (199.7) and Gd(DTPA–BDMA) (119.2) are close to that of GdDTPA (165.7), which indicates that these two complexes have favorable renal excretion capability like as GdDTPA. The renal excretion rates of Gd(cyclic-DTPA–1,2-pn), Gd(DTPA–BIN), and Gd(DTPA–BDEA) were much slower than that of GdDTPA, which can be useful for studying variations in organ blood volume and capillary permeability.[32] The low excretion rates of these agents in kidney are accompanied by that renal MRI intensity enhancement of these contrasts persisted during the imaging period.

The high variability of the percentage enhancement values in the different rats is most likely related to the different dose in the different rats due to the different body weight. The variability of the values is more valuable in clinical diagnosis as the same volume of contrast agents applies in the different body. The kidney is a very small structure, and partial volume effect[32] is probably responsible for its high variability of the percentage enhancement value as well.

The good stability, prominent water solubility, and the wide effective range of pH of the four GdDTPA bisamide derivatives presented in our previous experiments[33,34] are very profitable for the practical use of contrast agent.

Gd(DTPA–BDEA), Gd(DTPA–BIN), and Gd(cyclic-DTPA–1,2-pn) exhibit a favorable tolerance profile. The intravenous LD_{50} correlate well with the osmotic load, indicating that the complexes are relatively inert and long-term toxicity is unlikely.

Conclusion

Four neutral Gd-DTPA bis (amide) derivatives, Gd(DTPA–BDMA), Gd(DTPA–BDEA), Gd(DTPA–BIN), and Gd(cyclic-DTPA-1, 2-pn), were synthesized and evaluated by in vivo and in vitro experiments as the candidates of tissue-specific and low-osmolality MRI contrast agents. The measured relaxivities for Gd(DTPA–BDMA), Gd(DTPA–BDEA), Gd(DTPA–BIN), and Gd(cyclic-DTPA–1, 2-pn) in D_2O, bovine serum albumin and human serum transferrin showed favorable relaxation ability and binding ability with BSA and hTF. Our preliminary in vitro and in vivo studies on Gd(DTPA–BDMA), Gd(DTPA–BIN), and Gd(cyclic-DTPA–1, 2-pn) have proven that these three agents could be promising liver-specific MRI contrast agents and Gd(DTPA–BDMA), and Gd(cyclic-DTPA–1, 2-pn) have favorable renal excretion capability. Among them, Gd(cyclic-DTPA–1, 2-pn) is a more powerful hepatic contrast agent and Gd(DTPA–BIN) provides the stable imaging contrast for several hours. These agents (1) are well soluble in water suitable enough to be injected in an in vivo experiment; (2) display a higher relaxivity than that of the widely used contrast agent (GdDTPA); (3) show a long residence time in the body; (4) induce strong signal enhancement ability in liver; and (5) showed a lower toxicity.

Experimental

All commercial reagents were used directly without further purification unless specially notified. Elemental analyses were performed on a Vario EL elemental analyzer. NMR spectra were recorded on a Varian Unity-400 spectrometer.

Syntheses of ligands

DTPA–BDMA, DTPA–BDEA, and DTPA–BIN were synthesized by reacting DTPA-bisanhydride with the corresponding amine or hydrazide using the method for the synthesis of DTPA-bis-ethylamide.[24,35] Cyclic-DTPA–1, 2-pn was synthesized by analogous procedure to references.[36,37] The assignments in the ^1H and ^{13}C NMR spectra were based on related literatures.[9,36,38–40] Their structures were shown in Figure. 7.

DTPA–BDMA. 35.7 g (0.1 mol) of diethylenetriaminepentaacetic (DTPA) dianhydride was dissolved in 100 mL of dimethyl sulfoxide (DMSO). An excess of dimethylamide passed the solution during stirring until the color of solution changed from ashen to salmon pink. After additional 3 h, the reaction mixture was evaporated in a beaker at a temperature below 80 °C for the release of the excess dimethylamide and then allowed to cool. To the resulting mixture 700 mL of ethanol/ether (2/5) was added and left to stand for

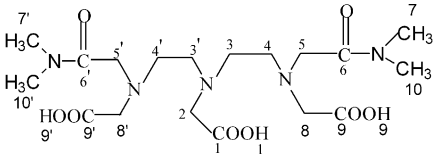

(a) DTPA-BDMA

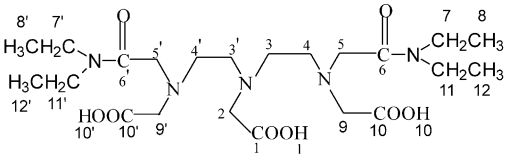

(b) DTPA-BDEA

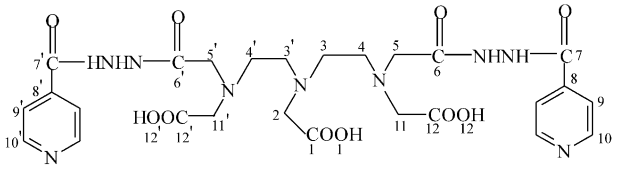

(c) DTPA-BIN

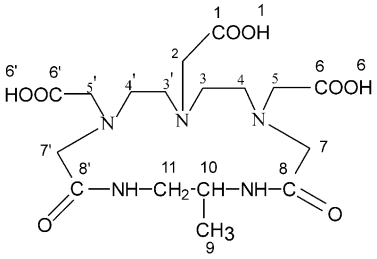

(d) cyclic-DTPA-1,2-pn

Figure 7. Structure and abbreviated name of DTPA-bisamide derivatives.

several days at room temperature. After filtration and wash thrice with ethanol/ether, the resulting solid was dried in vacuo at 54–58 °C and DTPA–BDMA was obtained as a white amorphous solid (yield 74.6%). ^{1}H NMR (399.94 MHz, D_2O, pH 2.92, 25 °C): δ 2.98 (s, 12H, H7, H7′, H10 and H10′), 3.10 (t, $^3J_{H,H}$ = 6.2 Hz, 4H, H3 and H3′), 3.49 (t, $^3J_{H,H}$ = 6.2 Hz, 4H, H4 and H4′), 3.52 (s, 2H, H2), 3.90 (s, 4H, H8 and H8′), 4.38 (s, 4H, H5 and H5′); ^{13}C NMR (100.58 MHz, D_2O, pH 2.92, 25 °C): δ 37.24 (C10 and C10′), 38.12 (C7 and C7′), 51.93 (C4 and C4′), 53.39 (C3 and C3′), 56.79 (C2), 57.15 (C8 and C8′), 59.64 (C5 and C5′), 174.07 (C9 and C9′), 179.02 (C6 and C6′), 179.83 (C1). Anal. calcd (found) for $C_{18}H_{33}N_5O_8$: C, 48.29 (48.11); H, 7.43 (7.37); N, 15.65 (15.77)%.

DTPA–BDEA. 35.7 g (0.1 mol) of DTPA dianhydride was dissolved in 60 mL of DMSO. A 10% excess of ethylenediamine (22.8 mL, 0.22 mol) was added dropwise and the mixture was stirred overnight at ambient temperature until the color of the solution changed to salmon pink. The reaction mixture was heated at 40 °C for about 20 h and then evaporated at a temperature below 80 °C for the removal of the excess ethylenediamine. To the cooling mixture 60 mL of ethanol was added and left to stand for several days at room temperature. After filtration and wash thrice with ethanol, the resulting solid was dried in vacuo at 55 °C and DTPA–BDEA was obtained as a white amorphous solid (yield 63.8%). ^{1}H NMR (399.94 MHz, D_2O, pH ~3.0, 25 °C): δ = 1.12 (t, $^3J_{H,H}$ = 7.2 Hz, 6H, H12 and H12′), 1.17 (t, $^3J_{H,H}$ = 7.7 Hz, 6H, H8 and H8′), 3.02 (t, $^3J_{H,H}$ = 6.0 Hz, 4H, H3 and H3′), 3.22 (q, $^3J_{H,H}$ = 7.2 Hz, 4H, H11 and H11′), 3.33 (q, $^3J_{H,H}$ = 7.7 Hz, 4H, H7 and H7′), 3.40 (t, $^3J_{H,H}$ = 6.0 Hz, 4H, H4 and H4′), 3.43 (s, 2H, H2), 3.82 (s, 4H, H9 and H9′), 4.28 (s, 4H, H5 and H5′); ^{13}C NMR (100.58 MHz, D_2O, pH ~3.0, 25 °C): δ = 13.58 (C12 and C12′), 14.50 (C8 and C8′), 42.73 (C11 and C11′), 43.26 (C7 and C7′), 50.65 (C4 and C4′), 54.93 (C3 and C3′), 55.59 (C2), 57.47 (C9 and C9′), 58.87 (C5 and C5′), 165.65 (C10 and C10′), 171.30 (C6 and C6′), 175.48 (C1). Anal. calcd (found) for $C_{22}H_{41}N_5O_8$: C, 52.47 (52.46); H, 8.21 (8.08); N, 13.91 (13.64)%.

DTPA–BIN. 35.7 g (0.1 mol) of DTPA dianhydride was dissolved in 60 mL of DMSO. A 10% excess of isoniazide (2.2 g, 0.22 mol) dissolved in DMSO was added dropwise. The mixture stirred for additional 12 h at ambient temperature. To the reaction mixture, 100 mL of anhydrous ethanol was added and left to stand for 6 h. After filtration and drying in vacuo, DTPA–BIN was obtained as a light yellow amorphous solid (yield 75.0%). ^{1}H NMR (399.94 MHz, D_2O, pH 3.41, 25 °C): δ = 3.25 (t, $^3J_{H,H}$ = 5.6 Hz, 4H, H3 and H3′), 3.47 (t, $^3J_{H,H}$ = 5.6 Hz, 4H, H4 and H4′), 3.61 (s, 4H, H11 and H11′), 3.75 (s, 4H, H5 and H5′), 3.89 (s, 2H, H2), 7.94 (d, $^3J_{H,H}$ = 6.0 Hz, 4H, H9 and H9′), 8.75 (d, $^3J_{H,H}$ = 6.0 Hz, 4H, H10 and H10′); ^{13}C NMR (100.58 MHz, D_2O, pH 3.41, 25 °C): δ = 51.67 (C3 and C3′), 54.91 (C4 and C4′), 56.53 (C2), 59.07 (C11 and C11′), 59.92 (C5 and C5′), 123.51 (C9 and C9′), 141.40 (C8 and C8′), 151.23 (C10 and C10′), 168.40 (C12 and C12′), 172.43 (C1), 174.51 (C7 and C7′), 180.58 (C6 and C6′). Anal. calcd (found) for $C_{26}H_{33}N_9O_{10}$: C, 49.44 (49.20); H, 5.27 (5.43); N, 19.96 (19.81)%.

Cyclic-DTPA–1,2-pn. To 6.35 g of DTPA dianhydride suspended in 500 mL of dimethylformamide (DMF) was added dropwise a DMF solution (50 mL) containing 1.52 mL of 1,2-propane diamide with vigorous stirring for 12 h. The reaction mixture was heated at 55 °C for additional 6 h and allowed to cool, then it was left to stand overnight at room temperature. The precipitate formed was removed by filtration. Concentration of the filtrate at a temperature below 40 °C resulted in the formation of a light yellow viscous liquid. When the resulting solution was mixed with 100 mL of tetrahydrofuran (THF), a light yellow solid was obtained. After filtration and drying in vacuo, the solid that was suspended in THF was heated at 50 °C with stirring for

2 h. A white solid was obtained after cooling, filtration and drying in vacuo at 80 °C, the resulting solid was dissolved in a small amount of water, then filtrated and left to stand for the free volatilization of water. Cyclic-DTPA–1, 2-pn was obtained as a colorless crystal (yield 52.3%). ^{1}H NMR (399.94 MHz, D_2O, pH 4.14, 25 °C): $\delta = 1.15$ (d, $^1J_{H,H} = 6.8$ Hz, 3H, H9), 3.18 (m, 4H, H4 and H4′), 3.36 (m, 4H, H3 and H3′), 3.40 (d, 2H, H11), 3.44 (s, 2H, H5), 3.45 (s, 2H, H5′), 3.59 (s, 2H, H7), 3.57 (s, 2H, H7′), 3.75 (AB, $^3J_{AB} = 17.2$ Hz, 2H, H2), 4.12 (m, 1H, H10); ^{13}C NMR (100.58 MHz, D_2O, pH 4.14, 25 °C): $\delta = 18.81$ (C9), 31.30 (C11), 44.36 (C4), 47.01 (C4′), 52.38 (C3), 52.73 (C3′), 55.06 (C2), 55.81 (C5′), 56.40 (C5), 59.85 (C10), 60.17 (C7), 61.02 (C7′), 174.98 (C8), 176.07 (C8′), 180.52 (C1), 180.86 (C6 and C6′). Anal. calcd (found) for $C_{17}H_{29}N_5O_8$: C, 47.32 (47.07); H, 6.78 (6.61); N, 16.24 (16.53)%.

Syntheses of gadolinium(III) complexes

The gadolinium(III) complexes were obtained by mixing stoichiometric amount of $GdCl_3$ with the DTPA-bisamide derivatives solutions. Typically, the mixtures were stirred overnight, and then adjusted to pH 7.3 ± 0.1. No free Gd^{3+} was detected by using a standard colorimetric method (xylenol orange was used as an indicator in NaAc/HOAc buffer at pH 5.3).

In vitro relaxation measurements

The relaxivities (r_1, $mM^{-1} \cdot s^{-1}$) of the four gadolinium complexes were measured by using a standard inversion-recovery pulse sequence in D_2O (buffer at pH 7.3 ± 0.1 in $NaOH/NaH_2PO_4$), bovine serum albumin (BSA) (0.725 mmol·L^{-1}, in D_2O solution) and human serum transferrin (hTF) (35 μmol L^{-1}, in D_2O solution) solutions at 9.39 T and 25 °C, respectively. For each complex, five samples were prepared separately with a concentration varying between 0 and 5 mM. Their relaxivities were obtained from the linear regressions [the relaxation rates ($1/T_1$) vs complex concentration].

Toxicity study

The toxicity of the complexes was assessed by their median lethal dose (LD_{50}). The LD_{50} of Gd(DTPA–BDEA), Gd(DTPA–BIN), and Gd(cyclic-DTPA–1,2-pn) were estimated by single intravenous (tail vein) injection of different volumes of a 100 mmol L^{-1} solution at a rate of 2 mL/min in Kunming male and female mice (19–22 g). The animals were observed for 14 days after the injection.

In vivo animal imaging study

MR imaging in rats was carried out at 4.7 T on a Bruker BIOSPEC-47/30 MRI imager. A series of T_1-weighted images of abdomen were obtained after intravenous injection (tail vein) of a bolus of 0.02 mmol GdDTPA and its derivatives solutions in separate three male Sprague–Dawley (SD) rats (90–120 g), respectively. MRI signal intensity enhancement was monitored up to 90 min at an interval of 5 min. Axial imaging of 2-mm slice thickness was acquired by multi-slice multi-echo (MSME) techniques (no. of slices = 4 and no. of echoes = 2) using TR = 500 ms, the times of two echoes (TE) = 15 and 60 ms, four average scans. A field of view (FOV) 50×50 mm and a data matrix of 128×256 were employed.

Data analysis

A water tube was placed in the field of view as a phantom reference. Thus, intensity enhancement (*IE*) of region of interest (*ROI*) at time t is expressed by

$$IE = 100 \times \frac{ROI_t - ROI_0}{ROI_0} \tag{2}$$

where ROI_t corresponds to the normalized signal intensity measured at time t and ROI_0 is the normalized signal intensity for precontrast.

To understand the properties of the complexes better, we assume that the uptake and the excretion of these agents follow a simplified first order reaction. Therefore, the intensity enhancement (*IE*) in the T_1-weighted images may be expressed in eq 3.

$$IE_t = IE_{\max} \times \left[1 - e^{-t/t_{1/2}}\right] \tag{3}$$

where $t_{1/2}$ is the half lifetime of uptake or excretion. Since both uptake and the excretion take place simultaneously, the observed *IE* can be expressed as eq 4.

$$\begin{aligned} IE_{\text{obsd}} &= IE_{\text{uptake}} - IE_{\text{excretion}} \\ &= IE_{\max} \times \left[-e^{-t/t_{1/2},\text{uptake}} + \mathrm{e}^{-t/t_{1/2},\text{excretion}}\right] \end{aligned} \tag{4}$$

Acknowledgements

For financial support, we thank State Key Laboratory of Magnetic Resonance and Atomic and Molecular Physics of China and Science and Technology Foundation of Changchun. We also thank Dr. Shanrong Zhang, University of Texas at Dallas, for helpful discussions.

References and Notes

1. Lauffer, R. B. *Chem. Rev.* **1987**, *390*, 901.
2. Runge, V. M. *J. Magn. Reson. Imaging* **2000**, *12*, 205.
3. Shellock, F. G.; Kanal, E. *J. Magn. Reson. Imaging* **1999**, *10*, 477.
4. Caravan, P.; Ellison, J. J.; McMurry, T. J.; Lauffer, R. B. *Chem. Rev.* **1999**, *99*, 2293.
5. Zhang, S. R.; Sun, D. Y.; Li, X. Y.; Pei, F. K.; Liu, S. Y. *Fullerene Sci. Techn.* **1997**, *5*, 1635.

6. Wolfgang, S.; Sanjay, S.; Jan, P.; Ralph, W.; Mukesh, H.; William, M. S.; Peter, F. H. *J. Magn. Reson. Imaging* **1999**, *10*, 80.
7. Lucia, J. M. K.; Joost, D.; Rob, J. V. D. G.; Albert, D. R. *J. Magn. Reson. Imaging* **1999**, *10*, 170.
8. Susanne, O.; James, F.; Timothy, P. L. R.; Michael, F. W.; Kenneth, D. A.; Jeffry, S. M.; Mark, A. I.; Robert, C. B. *J. Magn. Reson. Imaging* **1998**, *8*, 799.
9. Bligh, S. W. A.; Chowdhury, A. H. M. S.; Kennedy, D.; Luchinat, C.; Parigi, C. *Magn. Reson. Med.* **1999**, *41*, 767.
10. Fulvio, U.; Silvio, A.; Pier, L. A.; Mauro, B.; Marino, B.; Christoph, D. H.; Giuseppe, E.; Maurizio, G.; Paola, P. *Inorg. Chem.* **1995**, *34*, 633.
11. Bradshaw, J. E.; Gillogly, K. A.; Wilson, L. J.; Kumar, K.; Wan, X. M.; Tweedle, M. F.; Hernandez, C.; Bryant, R. G. *Inorg. Chim. Acta* **1998**, *275*, 106.
12. Gahrouei, D. S.; Williams, M.; Rizvi, S.; Allen, B. J. *J. Magn. Reson. Imaging* **2001**, *14*, 169.
13. Duarte, M. G.; Gil, M. H.; Peters, J. A.; Colet, J. M.; Elst, L. V.; Muller, R. N.; Geraldes, C. F. G. C. *Bioconjugate Chem.* **2001**, *12*, 170.
14. Bretonniere, Y.; Mazzanti, M.; Pecaut, J.; Dunand, F. A.; Merbach, A. E. *Chem. Commun.* **2001**, 621.
15. Fossheim, R.; Dugstad, H.; Dahl, S. G. *Eur. J. Med. Chem.* **1995**, *30*, 539.
16. Yu, X.; Song, S. K.; Chen, J. J.; Scott, M. J.; Fuhrhop, R. J.; Hall, C. S.; Gaffney, P. J.; Wickline, S. A.; Lanza, G. M. *Magn. Reson. Med.* **2000**, *14*, 867.
17. Anelli, P. L.; Bertini, I.; Fragai, M.; Lattuada, L.; Luchinat, C.; Parigi, G. *Eur. J. Inorg. Chem.* **2000**, *2000*, 625.
18. Roberts, H. C.; Saeed, M.; Roberts, T. P. L.; Muhler, A.; Brasch, R. C. *J. Magn. Reson. Imaging* **1999**, *9*, 204.
19. Su, M. Y.; Wang, Z. H.; Carpenter, P. M.; Lao, X. Y.; Muhler, A.; Nalcioglu, O. *J. Magn. Reson. Imaging* **1999**, *9*, 177.
20. Hofman, M. B.; Henson, R. E.; Kovacs, S. J.; Fischer, S. E.; Lauffer, R. B.; Adzamli, K.; Becker, J. D.; Wickline, S. A.; Lorenz, C. H. *Mang. Reson. Med.* **1999**, *41*, 360.
21. Caravan, P.; Comuzzi, C.; Crooks, W.; McMurry, T. J.; Choppin, G. R.; Woulfe, S. R. *Inorg. Chem.* **2001**, *40*, 2170.
22. Wang, Y. M.; Cheng, T. H.; Liu, G. C.; Sheu, R. S. *J. Chem. Soc., Dalton Trans.* **1997**, 833.
23. Varadarajan, J. A.; Crofts, S. P.; Carvalho, J. F.; Fellmann, J. D.; Kim, S. H.; Chang, C. A.; Watson, A. D. *Invest. Radiol.* **1994**, *29*, S18.
24. Konings, M. S.; Dow, W. C.; Love, D. B.; Raymond, K. N.; Quay, S. C.; Rocklage, S. M. *Inorg. Chem.* **1990**, *29*, 1488.
25. Adzamli, K.; Toth, E.; Periasamy, M. P.; Koenig, S. H.; Merbach, A. E.; Adams, M. D. *Magn. Reson. Mater. Phys., Biol. Med.* **1999**, *8*, 163.
26. Wei, J.; Zhuo, R. *Zhongguo Xitu Xuebao* **1998**, *16*, 289.
27. Aukrust, A.; Raknes, A.; Sjogren, C. E.; Sydnes, L. K. *Acta Chem. Scand.* **1997**, *51*, 918.
28. Li, X. Y.; Li, X. J.; Zhang, S. R.; Pei, F. K. *Polyhedron* **1999**, *18*, 695.
29. Li, X. J.; Feng, J. H.; Li, X. Y.; Wu, Y. J.; Pei, F. K. *Chin. J. Anal. Chem.* **2000**, *28*, 269.
30. Meng, L. Post-doctoral Thesis, Changchun Institute of Applied Chemistry, Chinese Academy of Sciences, 1997.
31. Bligh, S. W. A.; Harding, C. T.; Sadler, P. J.; Bulman, R. A.; Bydder, G. M.; Pennock, J. M.; Kelly, J. D.; Latham, I. A.; Marriott, J. A. *Magn. Reson. Med.* **1991**, *17*, 516.
32. Li, K. C. P.; Quisling, R. G.; Armitage, F. E.; Richardson, D.; Mladinichin, C. *Magn. Reson. Imaging* **1992**, *10*, 439.
33. Zhang, S. R.; Ren, J. M.; Pei, F. K. *Acta Phys.-Chim. Sinica* **1995**, *11*, 199.
34. Li, X. J.; Feng, J. H.; Jing, F. Y.; Li, X. Y.; Pei, F. K. *Chin. J. Magn. Reson.* **1999**, *16*, 525.
35. Quay, S. C. US Patent. 4687659, 1987.
36. Inoue, M. B.; Navarro, R. E.; Inoue, M.; Fernando, Q. *Inorg. Chem.* **1995**, *34*, 6074.
37. Inoue, M. B.; Inoue, M.; Munoz, I.; Bruck, M. A.; Fernando, Q. *Inorg. Chim. Acta* **1993**, *209*, 29.
38. Jenkins, B. G.; Lauffer, R. B. *Inorg. Chem.* **1988**, *27*, 4730.
39. Rizkalla, E. N.; Choppin, G. R. *Inorg. Chem.* **1993**, *32*, 582.
40. Geraldes, C. F. G. C.; Urbano, A. M.; Hoefnagel, M. A.; Peters, J. A. *Inorg. Chem.* **1993**, *32*, 2426.